Radiology

Renal Perfusion 3-T MR Imaging:

A Comparative Study of Arterial Spin Labeling and Dynamic Contrast-enhanced Techniques[1]

Wen-Chau Wu, PhD
Mao-Yuan Su, PhD
Chin-Cheng Chang, MD
Wen-Yih Isaac Tseng, MD, PhD
Kao-Lang Liu, MD

Purpose: To investigate the feasibility of and correlation between arterial spin-labeling (ASL) and dynamic contrast material–enhanced (DCE) 3-T magnetic resonance (MR) imaging in the measurement of renal blood flow (RBF).

Materials and Methods: The review board approved this study. Nineteen healthy volunteers (seven women, 12 men; age range, 25–68 years) were recruited, and each provided written informed consent. MR imaging was performed with a 3-T whole-body system. Each subject underwent back-to-back ASL and DCE MR imaging. Ten runs of ASL imaging were performed by using the pseudocontinuous tagging scheme, and each run required an 18-second breath hold. For DCE imaging, a gadopentetate dimeglumine bolus (0.0125 mmol per kilogram of body weight) was administrated intravenously in all subjects except two; in the latter subjects, a 0.025 mmol/kg gadopentetate dimeglumine bolus was administered to evaluate the T1 saturation effect. RBF was quantified with both techniques and in both the cortex and the medulla. Agreement was evaluated for RBF measurements obtained with ASL imaging and those obtained with DCE imaging by using correlation analysis.

Results: RBF was apparently overestimated with 0.025 mmol/kg gadopentetate dimeglumine, which is a concentration that is commonly adopted for 1.5-T DCE. RBF was 227 mL/100 mL/min ± 30 (standard deviation) in the cortex and 101 mL/100 mL/min ± 21 in the medulla, as measured with ASL imaging, and 272 mL/100 mL/min ± 60 in the cortex and 122 mL/100 mL/min ± 30 in the medulla, as measured with DCE imaging. In the cortex, measurements obtained with ASL and DCE imaging exhibited a linear correlation ($r = 0.66$; statistical power, 0.8 at the 5% significance level) and fair agreement (intraclass correlation coefficient, 0.41).

Conclusion: ASL and DCE 3-T MR imaging are feasible in the quantification of cortical renal perfusion, yielding measurements that are correlated but not entirely comparable. Intermodality differences have yet to be solved.

©RSNA, 2011

Microvascular blood flow, or perfusion, is an important index of physiology and pathophysiology. Abnormal perfusion may be both the cause and the consequence of disease development (1,2). Thus, reliable perfusion measurement is desirable, as it may facilitate the investigation of physiology and function, the formulation of the diagnosis and prognosis of disease, and the planning and evaluation of treatment. In the kidneys, perfusion has been used to assess renal allograft nephropathy (3,4) and renal cell carcinoma (5,6).

Quantitative measurement of renal perfusion has been achieved with positron emission tomography (PET) (7,8), contrast material–enhanced computed tomography (CT) (9), and magnetic resonance (MR) imaging (3–6,10–12). As compared with its counterparts, perfusion MR imaging is less invasive when one considers exposure to radioactive isotopes and ionizing irradiation and is less dependent on variable anatomy of vasculature than is flow measurement derived from phase-contrast MR imaging (13). Arterial spin-labeling (ASL) (13) and dynamic contrast-enhanced (DCE) imaging (14) are two established perfusion MR imaging techniques. In ASL, the protons in the arterial blood feeding the organ of interest are magnetically tagged or labeled by radiofrequency pulses, usually through inversion, and then serve as an endogenous tracer. Image acquisition follows after a sufficient amount of time has passed to enable the tagged protons to reach the capillary bed and exchange with the protons of surrounding tissue. In practice, a control image in contrast to the mentioned tag image is obtained without the tagging preparation. The tag image is subtracted from the control image to remove signals of static tissue, yielding residual signal that is proportional to the local blood flow. In DCE MR imaging, a bolus of paramagnetic contrast media, usually composed of gadolinium chelates, is intravenously injected while images are rapidly and repeatedly acquired over a few minutes. The signal evolution that accompanies the passage of contrast media is then associated with the concentration-time curves of contrast media from which blood flow is calculated.

While 3-T MR imaging has become more common in the past few years because of the gain in signal-to-noise ratio (SNR), most renal perfusion studies in which MR imaging is used have been performed with a field strength of 1.5 T (3–5,10–12). Specifically, the longer longitudinal relaxation time constant (T1) of blood at 3 T benefits ASL imaging in that the labeled protons persist longer through the delivery route to the imaging region. The purpose of this study was to investigate the feasibility of and the correlation between ASL and DCE MR imaging in the measurement of renal blood flow (RBF) at the field strength of 3 T.

Materials and Methods

Subjects

This study was approved by the review board of the National Taiwan University Hospital. Nineteen healthy volunteers, including seven women (mean age, 41 years ± 15 [standard deviation]; age range, 25–64 years) and 12 men (mean age, 43 years ± 16; age range, 25–68 years), were recruited, and all subjects gave written informed consent. Each subject was given earplugs and placed on the gantry table in the supine position, head first, with both arms extended

Advances in Knowledge

- Arterial spin-labeling (ASL) and dynamic contrast material–enhanced (DCE) MR imaging enable correlated but not entirely comparable perfusion measurement of the renal cortex ($r = 0.66$, intraclass correlation coefficient = 0.41).

- Reliable perfusion measurement of the renal cortex is possible with pseudocontinuous ASL imaging, with 10 repetitions of 18-second breath holds.

- With 3-T MR imaging, a lower concentration of gadopentetate dimeglumine (0.0125 mmol per kilogram of body weight) than that used with 1.5-T MR imaging yields sufficient signal-to-noise ratio for measurement of renal perfusion in the cortex with the DCE technique, without incurring the T1 saturation effect.

- ASL and DCE imaging enable reliable perfusion measurement of the renal cortex (within-subject coefficient of variation, 7.9% and 9.6%, respectively).

Implications for Patient Care

- ASL and DCE MR imaging may enable reliable perfusion quantification in the renal cortex with little to no invasiveness.

- Measurement of renal blood flow with the DCE technique is more time efficient than measurement with the ASL technique (1 minute vs 5 minutes), but it demands a longer breath hold than that required for each repetition of ASL imaging (30 seconds vs 18 seconds).

- Cross-referencing ASL and DCE measurements of renal perfusion should be conducted with caution.

overhead, then the angiocatheter was connected to intravenous tubing. Each subject was instructed to inhale and hold his or her breath at the end of exhalation. The built-in respiratory belt was placed on each subject's upper abdomen to monitor respiration and the completeness of breath holding.

MR Imaging

All MR imaging was performed with a whole-body 3-T imager (Tim Trio; Siemens, Erlangen, Germany) by using the spine matrix coil and a flexible torso matrix coil for signal reception and the body coil for radiofrequency transmission. After scout and T2-weighted turbo spin-echo anatomic imaging, ASL images were obtained by using the pseudocontinuous labeling scheme (15,16), in which continuous labeling is mimicked by a series of short radiofrequency pulses, whereas control images were obtained by alternating the polarity of the radiofrequency pulses by 180°. Because pseudocontinuous ASL can be implemented by using body coil transmission and phased-array reception, it yields the optimal balance between labeling efficiency and signal-to-noise ratio as compared with the conventional pulsed and continuous labeling scheme (16). In this study, pseudocontinuous ASL imaging was based on a single-shot gradient-echo echo-planar readout (repetition time msec/echo time msec, 3000/17; labeling duration, 1.5 seconds; postlabeling delay, 1 second; section thickness, 6 mm; five coronal sections; field of view, 33–40 cm; in-plane matrix, 128 × 64; voxel size range, 2.6 × 5.2 × 6.0 mm to 3.1 × 6.2 × 6.0 mm; and generalized autocalibrating partially parallel acquisition acceleration factor, two). The labeling plane was axial and located 70–90 mm above the center of the imaging volume such that it was approximately perpendicular to the abdominal aorta. Ten runs of ASL were conducted, and each comprised six measurements; the first two measurements were discarded. Thus, the duration of the breath hold was no longer than 18 seconds. A break of 5–10 seconds was inserted between runs. It took no more than 5 minutes to complete ASL imaging. For

DCE imaging, gadopentetate dimeglumine (0.0125 mmol per kilogram of body weight) was injected at a rate of 4 mL/sec by using a power injector and followed by a 15-mL saline flush. Gadopentetate dimeglumine at a different concentration (0.025 mmol/kg) was injected in two subjects to test the effect of T1 saturation. These two subjects were excluded from statistical analysis because marked flow overestimation was observed. Saturation-recovery turbo fast low-angle shot imaging was used for image acquisition (section thickness, 8 mm; two coronal sections and one axial section; postsaturation delay, 150 msec; flip angle, 10°; in-plane matrix, 192 × 155; voxel size range, 1.7 × 2.1 × 8.0 mm to 2.1 × 2.6 × 8.0 mm; generalized autocalibrating partially parallel acquisition acceleration factor, two; echo time, 0.98 msec; 228 msec per section), which started five measurements before the injection of contrast media and lasted for 75 measurements afterward (effective repetition time, 834 msec). The first five measurements were discarded. Each subject was instructed to hold his or her breath as long as he or she could without motion and to gently exhale when breath holding was no longer possible. ASL imaging was always performed before DCE imaging in the back-to-back experiments (Figs 1, 2).

Reproducibility of ASL and DCE data was tested in four subjects by repeating the experiments after 2.5 hours. The mean half-life of the elimination phase of gadopentetate dimeglumine has been determined to be 1.58 hours ± 0.13 at concentrations of 0.1 and 0.25 mmol/kg (17). Given that we used a 10-fold lower concentration (0.0125 mmol/kg), the carryover effect is expected to be negligible after 2 hours.

Data Processing

All complex data were reconstructed online into magnitude images and then exported to a workstation for off-line postprocessing. Bulk motion and receiver sensitivity were corrected for individual series of images. Automated affine registration was performed to enable scaling in addition to translation and rotation and was followed with
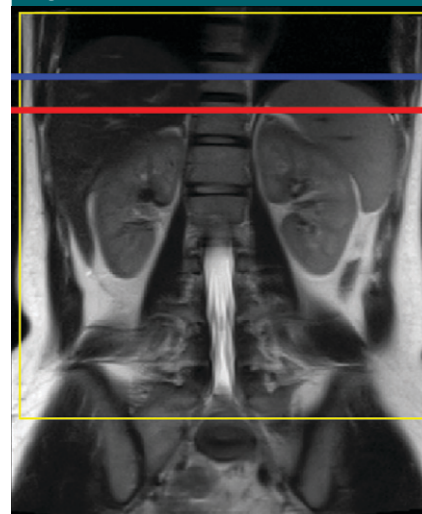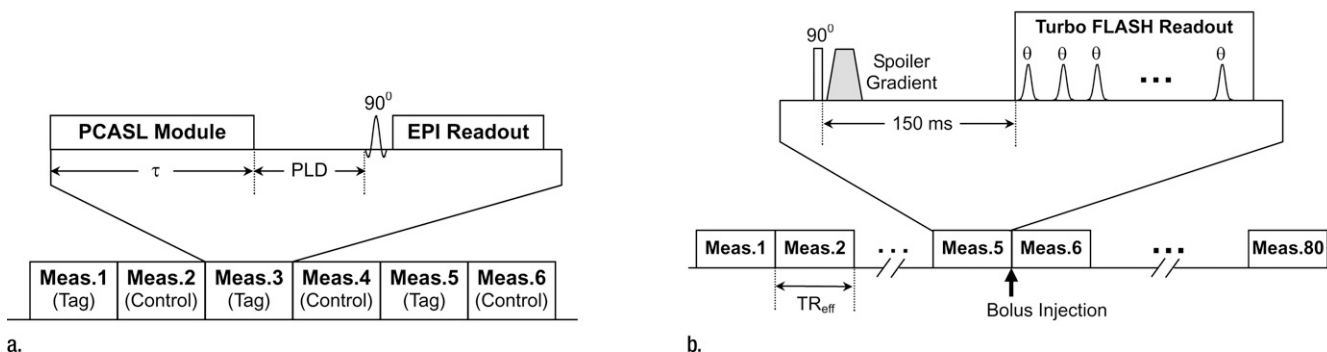
Figure 1: Section prescription for ASL and DCE half-Fourier rapid acquisition with relaxation enhancement MR imaging. Yellow box indicates one coronal section. Five coronal sections were acquired for ASL imaging, and two were acquired for DCE imaging. For DCE imaging, an axial section (red line) above the branch of renal arteries was also acquired for subsequent determination of arterial input function. For ASL imaging, the pseudocontinuous tagging and control planes (blue line) were placed 70–90 mm above the center of the imaging volume.

visual inspection, during which images with motion artifacts that could not be corrected with our algorithm were discarded (W.C.W., 7 years of experience in medical image processing). The tag and control images obtained with ASL imaging were subtracted in a pairwise manner, and an average was calculated to yield perfusion-weighted images (ΔM) that were converted to RBF maps by using the abdominal aorta as an internal reference to calculate the fully relaxed longitudinal magnetization of arterial blood (M_{0B}). We then used the cortex and medulla for the one-compartment model (18), with the assumption that by the time of image acquisition, all labeled protons had left the vessel and now resided in the parenchyma:

$$\mathrm{RBF_{ASL}} = \frac{\Delta M}{2\alpha M_{0B}\kappa \mathrm{T1_t}\left[\exp\left(-\dfrac{\mathrm{PLD}}{\mathrm{T1_t}}\right) - \exp\left(-\dfrac{\mathrm{PLD}+\tau}{\mathrm{T1_t}}\right)\right]},$$

[1]

Figure 2

Figure 2: Schematic diagrams of **(a)** ASL and **(b)** DCE MR imaging. ASL imaging consists of 10 repetitions of labeling duration *(τ)* of 1.5 msec and postlabeling delay *(PLD)* of 1 second. In **b**, the turbo fast low-angle shot *(FLASH)* readout includes two coronal sections and one axial section. *EPI* = echo-planar imaging, *Meas.* = measurement, *PCASL* = pseudocontinuous arterial spin labeling, *TR_eff* = effective repetition time.

where $\mathrm{RBF_{ASL}}$ is RBF measured with ASL imaging; $T1_t$ is T1 of the cortex or medulla (1150 and 1550 msec, respectively [19]); PLD is postlabeling delay; and τ is labeling duration,. Labeling efficiency (α) is assumed to be 0.75. To calculate κ, we used the equation $\kappa = \exp[(1/T1_t - 1/T1_b)\delta t]$, where $T1_b$ is T1 of the arterial blood (assumed to be 1600 msec) and δt is the transit time the tag took to travel from the tagging plane to the capillary bed. At 3-T MR imaging, κ was close to unity. This value was used throughout the study, implying a negligible transit time. To estimate transit time in the assessment of quantitative error, we referred to DCE imaging data, in which signal enhancement was observed in the kidneys no more than one frame (834 msec) after the abdominal aorta was enhanced. Thus, we estimated transit time to be 600 msec for the cortex and 800 msec for the medulla, leading to a worst-case overestimation of 15% and 2%, respectively. For DCE images, we used the following equation:

$$\mathrm{RBF_{DCE}} = [C_t(t) \otimes^{-1} C_a(t)]_{t=0}, \quad [2]$$

where $\mathrm{RBF_{DCE}}$ is RBF measured with DCE imaging and $\otimes^{-1}$ is the operation of deconvolution (20). $C_t(t)$ and $C_a(t)$ are the concentration-time curves of tissue (cortex or medulla) and the abdominal aorta (referred to as the arterial input function), respectively. Concentration-time curve ($C(t)$) was determined with the

following equation: $C(t) \propto (S(t) - S_0)/S_0$, where S_0 is the average signal intensity before arrival of the contrast agent and $S(t)$ is the signal-time curve (14,21). $C_a(t)$ was estimated on the axial section obtained through the abdominal aorta where a region of interest was placed carefully within the lumen to avoid partial volume effect. The time point where $C(t)$ started to increase was identified, which–along with the subsequent 30 time points–was fitted with a gamma variate function to remove second-pass or motion-related signal fluctuations. Block-circulant deconvolution (22) was adopted because of its insensitivity to the timing of bolus arrival. It is worth noting that the quantitative model implies that the capillary wall is infinitely permeable to gadopentetate dimeglumine when compared with the flow rate through the vessel.

Both kidneys in the section where they were seen most clearly were segmented into cortex and medulla with fuzzy c-means clustering of coregistered anatomic images and average dynamic images (echo-planar imaging for ASL imaging and saturation-recovery turbo fast low-angle shot for DCE imaging), from which average RBF was calculated for both kidneys on a per-subject basis.

Statistical Analysis

Reproducibility was assessed with within-subject coefficient of variation. An average was calculated for the two repetitions and then used for group analysis.

Agreement between RBF values measured with ASL imaging and those measured with DCE imaging was then evaluated in terms of inter- and intraclass correlation coefficients (r and ICC, respectively) and followed by Bland-Altman analysis. The interclass correlation coefficient was detected at the 5% significance level with the statistical power analyzed by using Fisher z transformation. For the ASL technique, spatial SNR was computed as the ratio of the mean in a target region of interest to the standard deviation in a background region of interest. For the DCE technique, temporal contrast-to-noise ratio (tCNR) was calculated from the signal-time curves with the equation $\mathrm{tCNR} = (S_p - S_b)/\sigma_b$ in which S_p is peak signal intensity and S_b and σ_b are the mean and standard deviation of baseline signal intensity, respectively. Postprocessing was performed with custom Matlab programs *(www.mathworks.com)*.

Results

Data collected in two subjects were excluded because of excessive motion, breath holding failure, or both. With DCE imaging, RBF was manifestly overestimated in the two subjects who received 0.025 mmol/kg gadopentetate dimeglumine (Fig 3) because of the convex relationship between DCE signal change and gadopentetate dimeglumine concentration. Although a linear approximation such as that used in
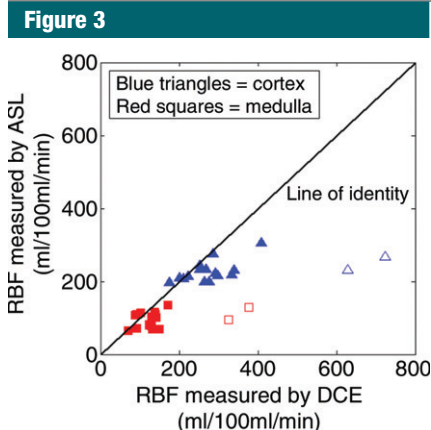
Figure 3

Figure 3: Scatterplot of RBF measured with ASL and DCE MR imaging. In the two volunteers who received 0.025 mmol/kg gadopentetate dimeglumine, RBF values obtained with DCE MR imaging were apparently overestimated (□ and △) and thus excluded from subsequent statistical analysis.

our model applies in the regimen of low concentration, the trend starts to saturate as concentration goes beyond a limit. This limit first appears in the arterial blood pool for a given bolus, leading to underestimation of arterial input function and thus overestimation of RBF (Equation [2]).

Figure 4 shows typical results of ASL and DCE MR imaging performed in one healthy volunteer.

DCE MR Imaging

Figure 4a and 4b shows DCE signal-time curves extracted from the kidneys, liver, and perinephric fat. The temporal contrast-to-noise ratio is 10.4 and 2.8 in the cortex and medulla, respectively. In the DCE RBF map (Fig 4c), the spurious hyperintensity of perinephric fat is due to failed model fitting because the signal fluctuations are irrelevant to the bolus passage.

ASL MR Imaging

In Figure 4d, no false perfusion was observed in perinephric fat. No perfusion was measured in the liver, most likely because of insufficient SNR, as the hepatic artery accounts for only 20% of liver perfusion. Also, because we did not always place the labeling plane well above the celiac trunk, the SNR may have been further compromised by low
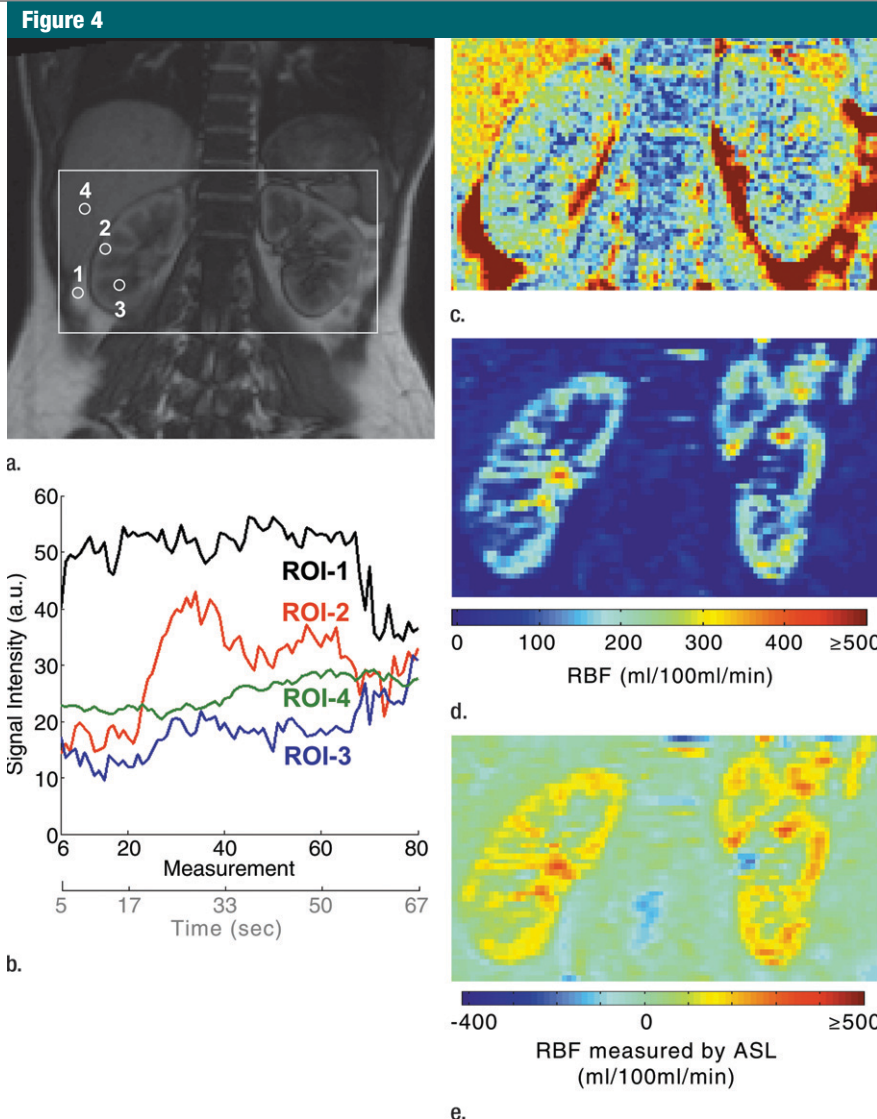
Figure 4

Figure 4: Measurement of RBF with ASL and DCE MR imaging. **(a)** Saturation-recovery turbo fast low-angle shot MR image shows four regions of interest (*1*, perinephric fat; *2*, renal cortex; *3*, renal medulla; and *4*, liver). **(b)** DCE MR imaging signal-time curves are shown for comparison. Regions of interest 1–4 (*ROI-1* through *ROI-4*) correspond to those in **a**. The interval between measurements (or effective repetition time) is 834 msec. **(c, d)** Subplots are quantitative RBF maps generated with **(c)** DCE and **(d)** ASL MR imaging. **(e)** Negative RBF values obtained with ASL MR imaging are preserved to assess spatial signal-to-noise ratio.

tagging efficiency as a result of tortuous geometry of the hepatic artery. Spatial SNR calculated against the background is 11.2 in the cortex and 3.4 in the medulla (Fig 4e).

Figure 5 is the scatterplot of RBF values measured with ASL versus those measured with DCE imaging ($n = 15$). A linear correlation was found between ASL and DCE measurements in the cortex ($r = 0.66$, $P = .05$, statistical power = 0.8, $RBF_{ASL} = 0.33 \times RBF_{DCE} + 137.07$) but not in the medulla ($r = 0.32$, $P = .25$). The Bland-Altman plots (Fig 6) show no effect of sample spread on the correlation. RBF_{DCE} is significantly higher than RBF_{ASL} in both the cortex and the medulla (paired *t* test, $P < .001$). The intraclass correlation coefficient was 0.41 in the cortex and 0.03 in the medulla. RBF_{ASL} was 227 mL/100 mL/min $\pm$ 30 in the cortex and
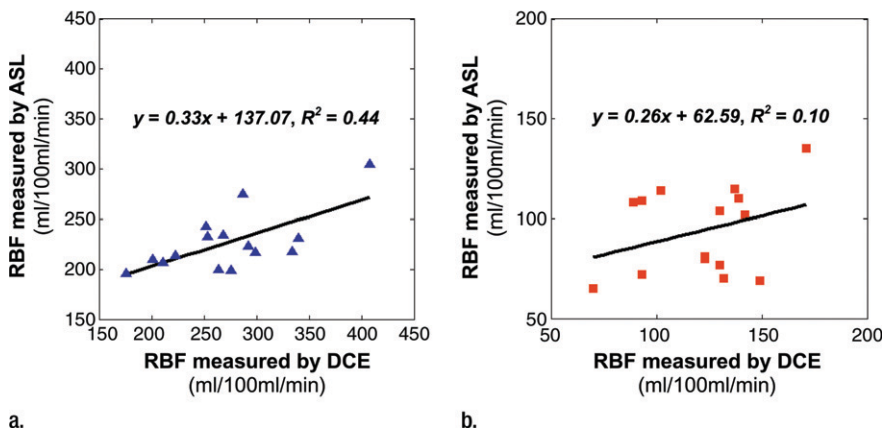
Figure 5

Figure 5: Scatterplots of RBF values obtained in the **(a)** cortex (▲) and **(b)** medulla (■) with ASL and DCE MR imaging.
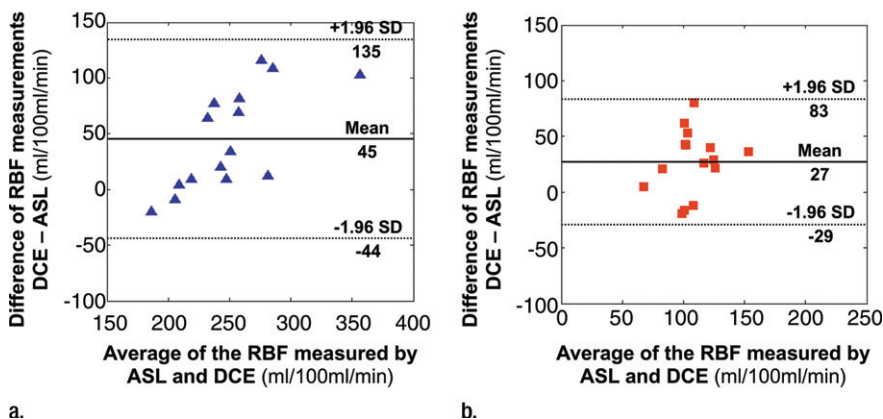
Figure 6

Figure 6: Bland-Altman plots of RBF values obtained in the **(a)** cortex (▲) and **(b)** medulla (■) with ASL and DCE MR imaging. Solid line denotes the mean, and dotted lines denote 1.96 standard deviation *(SD)* bounds.

101 mL/100 mL/min ± 21 in the medulla (n = 15). RBF$_{DCE}$ was 272 mL/100 mL/min ± 60 in the cortex and 122 mL/100 mL/min ± 30 in the medulla (n = 15). With the ASL technique, within-subject coefficient of variation was 7.9% in the cortex and 7.2% in the medulla. With the DCE technique, within-subject coefficient of variation was 9.6% in the cortex and 19.1% in the medulla.

Discussion

ASL and DCE MR imaging have been used to obtain RBF measurements in

several studies (3–6,10), although cross-modal comparison has been lacking. It may be difficult to refer to the documented results without knowing whether the flow values obtained with the two techniques can be interpreted interchangeably. In our study, head-to-head comparison was performed at 3 T to meet this need. Our results indicate that the renal perfusion values measured with ASL and DCE were correlated but not entirely comparable. Although ASL MR imaging and DCE MR imaging are feasible in the cortex, they are hindered in the measurement of perfusion in the

medulla by low SNR, low contrast-to-noise ratio, and incomplete quantitative models. It is also noted that for 3-T DCE MR imaging, the concentration of gadopentetate dimeglumine must be reduced from that used at 1.5 T to avoid flow overestimation.

Use of 3-T MR imaging is receiving attention because of the advances in hardware that make possible the theoretically predicted increase in SNR when compared with the SNR obtained with 1.5-T MR imaging. The change in field strength alters MR signal characteristics through varied spin properties. Specifically, the change of T1 can affect DCE imaging by shifting the adequate concentration of gadopentetate dimeglumine with which linear approximation remains appropriate for the association between the signal change against baseline and the contrast media concentration. Indeed, our experiments revealed that 0.025 mmol/kg gadopentetate dimeglumine, a concentration commonly used in 1.5-T MR imaging (0.02–0.05 mmol/kg), incurs signal saturation in the abdominal aorta where arterial input function is determined, leading to flow overestimation. The problem can be avoided by reducing the concentration to 0.0125 mmol/kg, as in this study, while SNR remains sufficient for cortical perfusion quantification. It is noteworthy that the contrast agent concentration we used does not afford optimal enhancement of anatomy or lesions. To acquire contrast-enhanced T1-weighted images, administration of additional contrast agent will be necessary after DCE imaging. Although more elaborate methods of calibrating the relationship between DCE signal change and gadopentetate dimeglumine concentration have been proposed (11,23), linear approximation has been proved to be simple yet realistic as long as the gadopentetate dimeglumine concentration does not exceed a limit to cause underestimation of the arterial input function (14,24).

RBF, as measured with ASL and DCE MR imaging in 15 healthy subjects was 227 mL/100 mL/min and 272 mL/100 mL/min, respectively, in the cortex and 101 mL/100 mL/min and 122 mL/100 mL/min, respectively, in the medulla;

these values were comparable with those in previous studies (10,11,25,26). However, we found that measurements obtained with ASL and DCE MR imaging lacked correlation ($r = 0.32$, $P = .25$) and consistency (ICC = 0.03) in the medulla. Thus, the flow values of the medulla should be interpreted with caution because the accuracy might have been compromised by two limitations: First, there was low signal-to-noise ratio and low contrast-to-noise ratio. While the SNR obtained with ASL MR imaging (<4.0) does not enable reliable separation of the medulla from the background, the temporal contrast-to-noise ratio of DCE MR imaging (<3.0) is marginal for robust deconvolution. Second, neither of the quantitative models that we adopted for ASL and DCE imaging accounts for the clearance of contrast material (water and gadopentetate dimeglumine) through medullary pyramids. As a result, the following discussion will be focused on cortical flow measurement.

With per-subject back-to-back ASL and DCE MR imaging, we have shown that these two techniques enable linearly correlated flow measurement in the renal cortex ($r = 0.66$, $P = .05$, statistical power = 0.8); however, the ASL technique tends to yield lower RBF measurements than does the DCE technique ($RBF_{ASL} = 0.33 \times RBF_{DCE} + 137.07$), yielding merely fair agreement between ASL and DCE findings (ICC = 0.41). This discrepancy could be the result of overestimation of RBF with the DCE technique because of residual signal saturation in the artery, error propagation from deconvolution, or both. The discrepancy could also be caused by underestimation of RBF_{ASL} due to unanticipated loss of tagging efficiency. Furthermore, the ASL model assumes retention of tags in the capillary bed; this is generally appropriate in the brain, but it may not be appropriate in the kidneys considering their high flow rate, the absence of a blood-brain barrier, and the filtration function. If tags leave the capillary bed before image acquisition and such loss is not accounted for, RBF_{ASL} will be underestimated. By using RBF_{DCE} as a reference standard,

about 15% of the tags were lost through glomerular filtration, outflow, or both. Because glomerular filtration rate is affected by factors such as age, sex, and body size, subject-wise correction for the effect is expected to improve the accuracy of RBF_{ASL}. Both the ASL and the DCE technique yield good precision (within-subject coefficient of variation, 7.9% and 9.6%, respectively).

Among various ASL methods, we adopted the pseudocontinuous labeling scheme because it offers an optimal balance between SNR and tagging efficiency (16), permitting RBF measurement with an examination time that is short and adequate for our purpose. Since our protocol requires breath holding, the duration of each individual imaging pass and of the total examination has to be short enough to allow each subject to hold his or her breath in a stable and consistent pattern. One caveat about pseudocontinuous labeling is that its labeling efficiency is susceptible to magnetic field inhomogeneity. This factor can be unfavorable to the free-breathing protocol for pseudocontinuous ASL measurement of RBF because the perturbed air in the abdomen may alter the labeling efficiency from measurement to measurement. In our study, we asked subjects to inhale first and then hold their breath at the end of exhalation. This may have reduced the variation of field homogeneity and thus the labeling efficiency between measurements. Nevertheless, the labeling efficiency is likely to deviate from the ideal value (approximately 85% [16]). To further reduce intersubject variability, labeling efficiency will need to be calibrated on a per-subject basis.

Another method with which to improve the stability of ASL signal is background suppression (27), in which two to four inversion pulses are applied before the excitation radiofrequency pulse for data readout. The timing of background suppression pulses is adjusted such that by the time of readout excitation, the static tissues of a predetermined range of T1 will be close to zero, while the flow contrast between tag and control images is preserved. We currently do not include background suppression in

our imaging protocol because of the increased specific absorption rate and loss of tags caused by nonideal inversion of background suppression pulses (28).

Respiratory motion is arguably a major challenge in abdominal MR imaging. In this regard, researchers (10) have suggested inclusion of respiratory gating to reduce motion-related degradation in image quality, data corruption, or both. While prospective gating prolongs examination time even in collaborative subjects and may become impractical in patients, retrospective gating entails extended measurement to collect enough images in the same phase of respiration. For ASL imaging, retrospective gating is advantageous in providing time-efficient measurements at multiple respiratory phases as compared with prospective gating. However, if one wishes only to measure RBF without regard to separation of respiratory phases, the long examination time is unnecessary. In our experience with multiple breath holds, reliable RBF measurements can be obtained with pseudocontinuous ASL imaging in 5 minutes with interexamination rest included. However, it should be noted that the newly proposed pseudocontinuous labeling scheme offers a 50% increase in SNR as compared with conventional pulsed ASL (16). On the basis of the square root relationship between SNR and the number of signals acquired, if one wishes to obtain the same SNR as in our experiment by using pulsed ASL, the examination time will have to be doubled (approximately 10 minutes). In that case, repeated breath holding is less desirable, as the imaging time is comparable to the length when one uses retrospective gating (12). For DCE MR imaging, respiratory gating is incompatible with the requirement of tracking the contrast agent passage. Fortunately, the kidneys are well perfused, and the first pass of the contrast agent usually arrives within 15 seconds after injection and peaks no later than 20 seconds thereafter. A breath hold of approximately 30 seconds can be endured by most subjects; however, this may not always be possible in all patients.

A few limitations of this study should be noted. First, we opted for affine registration to remove bulk motion. To cope with nonrigid body deformation, as is typical in abdominal imaging, nonlinear transformation, such as the elastic model, should be more appropriate; however, it may be more expensive in computation. Second, the models we adopted for flow quantification do not account for glomerular filtration and contrast agent clearance through the medullary pyramids. Modification of the models to include these factors should improve the accuracy of quantification. Third, the labeling efficiency of pseudocontinuous ASL has not been calibrated, even though it has been shown to be susceptible to field inhomogeneity. A few methods (29–32) have been proposed to correct this effect at the expense of additional imaging time. Fourth, we had no real reference standard. We could only compare the two methods, each of which has inaccuracies, with each other.

Accumulated evidence has revealed a causal relationship between nephrogenic systemic fibrosis and the use of gadopentetate dimeglumine in subjects with incomplete or impaired renal function (33,34). However, as long as the subject's renal function is carefully tested before he or she is exposed to contrast media, DCE MR imaging is still a useful technique with which to obtain RBF measurements with minimal invasiveness as compared with PET and contrast-enhanced CT. ASL MR imaging enables us to measure RBF noninvasively, and it is suitable for use in all subjects who are eligible for MR imaging; however, its inherently low SNR may be a limiting factor in some subjects. Although we have shown that ASL and DCE 3-T MR imaging are feasible in measuring cortical renal perfusion, nontrivial discrepancies remain between the flow values obtained with the two techniques. Further investigation is needed with regard to biophysical modeling, SNR improvement, and motion correction.

References

1. Azar S, Johnson MA, Hertel B, Tobian L. Single-nephron pressures, flows, and resistances in hypertensive kidneys with nephrosclerosis. Kidney Int 1977;12(1):28–40.

2. Zierler RE, Bergelin RO, Davidson RC, Cantwell-Gab K, Polissar NL, Strandness DE Jr. A prospective study of disease progression in patients with atherosclerotic renal artery stenosis. Am J Hypertens 1996; 9(11):1055–1061.

3. Pereira RS, Gonul II, McLaughlin K, Yilmaz S, Mahallati H. Assessment of chronic renal allograft nephropathy using contrast-enhanced MRI: a pilot study. AJR Am J Roentgenol 2010;194(5):W407–W413.

4. Lanzman RS, Wittsack HJ, Martirosian P, et al. Quantification of renal allograft perfusion using arterial spin labeling MRI: initial results. Eur Radiol 2010;20(6):1485–1491.

5. Notohamiprodjo M, Sourbron S, Staehler M, et al. Measuring perfusion and permeability in renal cell carcinoma with dynamic contrast-enhanced MRI: a pilot study. J Magn Reson Imaging 2010;31(2):490–501.

6. De Bazelaire C, Rofsky NM, Duhamel G, Michaelson MD, George D, Alsop DC. Arterial spin labeling blood flow magnetic resonance imaging for the characterization of metastatic renal cell carcinoma(1). Acad Radiol 2005;12(3):347–357.

7. Alpert NM, Rabito CA, Correia DJ, et al. Mapping of local renal blood flow with PET and H(2)(15)O. J Nucl Med 2002;43(4):470–475.

8. Anderson H, Yap JT, Wells P, et al. Measurement of renal tumour and normal tissue perfusion using positron emission tomography in a phase II clinical trial of razoxane. Br J Cancer 2003;89(2):262–267.

9. Fournier LS, Oudard S, Thiam R, et al. Metastatic renal carcinoma: evaluation of anti-angiogenic therapy with dynamic contrast-enhanced CT. Radiology 2010;256(2):511–518.

10. Gardener AG, Francis ST. Multislice perfusion of the kidneys using parallel imaging: image acquisition and analysis strategies. Magn Reson Med 2010;63(6):1627–1636.

11. Vallée JP, Lazeyras F, Khan HG, Terrier F. Absolute renal blood flow quantification by dynamic MRI and Gd-DTPA. Eur Radiol 2000;10(8):1245–1252.

12. Robson PM, Madhuranthakam AJ, Dai W, Pedrosa I, Rofsky NM, Alsop DC. Strategies for reducing respiratory motion artifacts in renal perfusion imaging with arterial spin labeling. Magn Reson Med 2009;61(6):1374–1387.

13. Detre JA, Zhang W, Roberts DA, et al. Tissue specific perfusion imaging using arterial spin labeling. NMR Biomed 1994;7(1-2):75–82.

14. Brix G, Semmler W, Port R, Schad LR, Layer G, Lorenz WJ. Pharmacokinetic parameters in CNS Gd-DTPA enhanced MR imaging. J Comput Assist Tomogr 1991;15(4):621–628.

15. Garcia DM, de Bazelaire C, Alsop D. Pseudocontinuous flow driven adiabatic inversion for arterial spin labeling [abstr]. In: Proceedings of the Thirteenth Meeting of the International Society for Magnetic Resonance in Medicine. Berkeley, Calif: International Society for Magnetic Resonance in Medicine, 2005; 37.

16. Wu WC, Fernández-Seara M, Detre JA, Wehrli FW, Wang J. A theoretical and experimental investigation of the tagging efficiency of pseudocontinuous arterial spin labeling. Magn Reson Med 2007;58(5):1020–1027.

17. Weinmann HJ, Laniado M, Mützel W. Pharmacokinetics of GdDTPA/dimeglumine after intravenous injection into healthy volunteers. Physiol Chem Phys Med NMR 1984;16(2):167–172.

18. Wu WC, Wang J, Detre JA, et al. Hyperemic flow heterogeneity within the calf, foot, and forearm measured with continuous arterial spin labeling MRI. Am J Physiol Heart Circ Physiol 2008;294(5):H2129–H2136.

19. de Bazelaire CM, Duhamel GD, Rofsky NM, Alsop DC. MR imaging relaxation times of abdominal and pelvic tissues measured in vivo at 3.0 T: preliminary results. Radiology 2004;230(3):652–659.

20. Jerosch-Herold M, Swingen C, Seethamraju RT. Myocardial blood flow quantification with MRI by model-independent deconvolution. Med Phys 2002;29(5):886–897.

21. Jerosch-Herold M, Wilke N. MR first pass imaging: quantitative assessment of transmural perfusion and collateral flow. Int J Card Imaging 1997;13(3):205–218.

22. Wu O, Østergaard L, Weisskoff RM, Benner T, Rosen BR, Sorensen AG. Tracer arrival timing-insensitive technique for estimating flow in MR perfusion-weighted imaging using singular value decomposition with a block-circulant deconvolution matrix. Magn Reson Med 2003;50(1):164–174.

23. Materne R, Smith AM, Peeters F, et al. Assessment of hepatic perfusion parameters with dynamic MRI. Magn Reson Med 2002; 47(1):135–142.

24. Wolf GL, Hoop B, Cannillo JA, Rogowska JA, Halpern EF. Measurement of renal transit

Radiology

of gadopentetate dimeglumine with echo-planar MR imaging. J Magn Reson Imaging 1994;4(3):365–372.

25. Martirosian P, Klose U, Mader I, Schick F. FAIR true-FISP perfusion imaging of the kidneys. Magn Reson Med 2004;51(2):353–361.

26. Fenchel M, Martirosian P, Langanke J, et al. Perfusion MR imaging with FAIR true FISP spin labeling in patients with and without renal artery stenosis: initial experience. Radiology 2006;238(3):1013–1021.

27. Ye FQ, Frank JA, Weinberger DR, McLaughlin AC. Noise reduction in 3D perfusion imaging by attenuating the static signal in arterial spin tagging (ASSIST). Magn Reson Med 2000;44(1):92–100.

28. Garcia DM, Duhamel G, Alsop DC. Efficiency of inversion pulses for background

suppressed arterial spin labeling. Magn Reson Med 2005;54(2):366–372.

29. Jung Y, Wong EC, Liu TT. Multiphase pseudocontinuous arterial spin labeling (MP-PCASL) for robust quantification of cerebral blood flow. Magn Reson Med 2010; 64(3):799–810.

30. Luh WM, Talagala SL, Bandettini PA. Robust prescan for pseudo-continuous arterial spin labeling at 7T: Estimation and correction for off-resonance effects [abstr]. In: Proceedings of the Eighteenth Meeting of the International Society for Magnetic Resonance in Medicine. Berkeley, Calif: International Society for Magnetic Resonance in Medicine, 2010; 520.

31. Jahanian H, Noll DC, Hernandez-Garcia L. Optimizing the inversion efficiency of pseudo-continuous ASL pulse sequence using B0 field map information [abstr]. In: Proceed-

ings of the Eighteenth Meeting of the International Society for Magnetic Resonance in Medicine. Berkeley, Calif: International Society for Magnetic Resonance in Medicine, 2010; 519.

32. Wu WC, Jiang SF, Yang SC, Lien SH. Pseudocontinuous arterial spin labeling perfusion magnetic resonance imaging—a normative study of reproducibility in the human brain. Neuroimage 2011;56(3):1244–1250.

33. Sam AD 2nd, Morasch MD, Collins J, Song G, Chen R, Pereles FS. Safety of gadolinium contrast angiography in patients with chronic renal insufficiency. J Vasc Surg 2003;38(2): 313–318.

34. Bongartz G, Mayr M, Bilecen D. Magnetic resonance angiography (MRA) in renally impaired patients: when and how. Eur J Radiol 2008;66(2):213–219.